THE JOURNAL OF BIOLOGICAL CHEMISTRY VOL. 289, NO. 43, pp. 29665–29676, October 24, 2014

MicroRNA-539 Is Up-regulated in Failing Heart, and Suppresses *O*-GlcNAcase Expression*

Received for publication, May 5, 2014, and in revised form, August 27, 2014 Published, JBC Papers in Press, September 2, 2014, DOI 10.1074/jbc.M114.578682

Senthilkumar Muthusamy, Angelica M. DeMartino, Lewis J. Watson, Kenneth R. Brittian, Ayesha Zafir, Sujith Dassanayaka, Kyung U. Hong, and Steven P. Jones[1]

From the Institute of Molecular Cardiology, and, Diabetes and Obesity Center, University of Louisville, Louisville, Kentucky 40202

Background: Protein *O*-GlcNAcylation is nearly ubiquitous; however, regulation of the expression of key enzymes remains unknown.
Results: miR-539 is up-regulated in the failing heart, binds to the 3′UTR, and negatively regulates *O*-GlcNAcase expression.
Conclusion: Protein *O*-GlcNAcylation can be regulated by post-transcriptional mechanisms.
Significance: miR-539 regulates one of the two enzymes responsible for *O*-GlcNAcylation in multicellular eukaryotes.

Derangements in metabolism and related signaling pathways characterize the failing heart. One such signal, *O*-linked β-*N*-acetylglucosamine (O-GlcNAc), is an essential post-translational modification regulated by two enzymes, *O*-GlcNAc transferase and *O*-GlcNAcase (OGA), which modulate the function of many nuclear and cytoplasmic proteins. We recently reported reduced OGA expression in the failing heart, which is consistent with the pro-adaptive role of increased *O*-GlcNAcylation during heart failure; however, molecular mechanisms regulating these enzymes during heart failure remain unknown. Using miRNA microarray analysis, we observed acute and chronic changes in expression of several miRNAs. Here, we focused on miR-539 because it was predicted to target OGA mRNA. Indeed, co-transfection of the OGA-3′UTR containing reporter plasmid and miR-539 overexpression plasmid significantly reduced reporter activity. Overexpression of miR-539 in neonatal rat cardiomyocytes significantly suppressed OGA expression and consequently increased *O*-GlcNAcylation; conversely, the miR-539 inhibitor rescued OGA protein expression and restored *O*-GlcNAcylation. In conclusion, this work identifies the first target of miR-539 in the heart and the first miRNA that regulates OGA. Manipulation of miR-539 may represent a novel therapeutic target in the treatment of heart failure and other metabolic diseases.

Heart failure is a multifactorial process and, despite some advances, few effective treatments have emerged in the last two decades. During heart failure, the myocardium undergoes profound alterations in gene expression and metabolic substrate utilization, which are associated with both pro- and maladaptive changes in mechanics and energetics (1). Likewise, nutrient and stress sensing mechanisms are also implicated, although debate still rages regarding what, exactly, such changes mean to the pathology or recovery of the failing heart.

At the cellular level, an ever-growing list of post-translational modifications affects organ function. Of these numerous post-translational modifications, *O*-linked *N*-acetylglucosamine (O-GlcNAc)[2] modification of proteins represents an emerging target in various pathologies (2, 3). The hexosamine biosynthetic pathway forms UDP-*N*-acetylglucosamine (UDP-GlcNAc), which serves as the sugar donor for the O-GlcNAc modification. Two antagonistic enzymes, *O*-GlcNAc transferase (OGT) and *O*-GlcNAcase (OGA; human gene: MGEA5), directly regulate *O*-GlcNAcylation of proteins inasmuch as OGT catalyzes the addition of GlcNAc to some serine and/or threonine residues in proteins, whereas OGA removes it. Altered levels of *O*-GlcNAcylation occur in many pathological conditions, including cardiovascular disease, diabetes mellitus, neurodegeneration, and cancer (4–6).

Disruption of blood flow (*i.e.* ischemia) induces metabolic and oxidative stress to the myocardium. Various *in vitro* studies of isolated cells/hearts showed elevated *O*-GlcNAc levels in response to various stressors (4, 7, 8). Moreover, augmented *O*-GlcNAcylation improved cell survival in various model systems (9, 10). Recently, our laboratory demonstrated that *O*-GlcNAcylation was increased in an infarct-induced heart failure model, which was associated with increased expression of OGT and reduced OGA expression (11). Although there are plausible metabolic explanations that may partially explain increased *O*-GlcNAc levels in failing hearts, other possibilities exist.

Although many regard flux of substrate through the hexosamine biosynthetic pathway as the only (or at least primary) mechanism regulating *O*-GlcNAcylation, other regulatory mechanisms remain unexplored. Thus, understanding the mechanisms regulating expression of OGT and OGA persist as important limitations in the field. One potential area of molecular regulation may involve microRNAs (miRNAs), which are endogenous small RNAs (~22 nucleotides) that play key regulatory roles in

* This work was supported, in whole or in part, by National Institutes of Health Grants R01 HL083320, R01 HL094419, P20 RR024489, P01 HL078825, and R37 HL055757 (to S. P. J.) and American Heart Association Predoctoral (Great Rivers Affiliate) Fellowship 0815502D (to L. J. W.).
[1] To whom correspondence should be addressed: 580 South Preston St., 321F Delia Baxter Building, Louisville, KY 40202. E-mail: Steven.P.Jones@Louisville.edu.

[2] The abbreviations used are: *O*-GlcNAc, *O*-linked *N*-acetylglucosamine; OGT, *O*-GlcNAc transferase; OGA, *O*-GlcNAcase; MI, myocardial infarction; miRNA, microRNA; NRCMs, neonatal rat cardiomyocytes; qRT, quantitative RT; BisTris, 2-[bis(2-hydroxyethyl)amino]-2-(hydroxymethyl)propane-1,3-diol; mmu, mus musculus.

fine-tuning gene expression by ultimately inhibiting translation of their target mRNAs and such post-transcriptional regulation has been associated with various cardiovascular diseases (12–14). Emerging evidence indicates that the miRNA expression profile changes in a region-specific manner during myocardial ischemia (15). Several diseases, at least experimentally, are improved by oligonucleotide-based technologies, making them attractive therapeutic candidates. Here we hypothesize that miRNAs up-regulated in heart failure may suppress OGA. The combination of miRNA microarray and bioinformatics revealed miR-539 as a potential novel regulator of OGA expression. These findings have important implications for cardiovascular disease, diabetes, metabolism, and other conditions in which alterations in *O*-GlcNAcylation may be implicated.

EXPERIMENTAL PROCEDURES

Myocardial Infarction—Adult (3–4 months old) C57BL6/J mice were subjected to *in vivo* coronary ligation to induce heart failure, as described previously (11, 16–20). In brief, mice were orally intubated, subjected to a thoracotomy, and the left coronary artery visualized and permanently occluded with the aid of a dissecting microscope. Upon recovery of spontaneous respiration, the endotracheal tube was removed and mice were allowed to recover in a temperature-controlled area supplemented with oxygen. All animal procedures were performed in accordance with federal guidelines and approved by the University of Louisville Animal Care and Use Committee.

Echocardiographic Assessment—Transthoracic echocardiography of the left ventricle was performed as previously described (16, 21, 22). Body temperature was maintained at 36.5–37.5 °C using a rectal thermometer interfaced with a servo-controlled heat lamp throughout the procedure. Briefly, mice were anesthetized with 2% isoflurane then maintained under anesthesia with 1.5% isoflurane and examined. Using the Vevo rail system, the mouse was placed chest up on an examination board interfaced with the Vevo 770. Next, depilatory cream was applied to the chest of the mouse and wiped clean to remove all hair in the area of interest. The 707-B (30 MHz) scan head was used to obtain two-dimensional images (100 frames/s) of the parasternal long axis. M-modes images were also acquired. The probe was then rotated to acquire a short axis view of the heart. Beginning at the level of the papillary muscles and moving apically, serial two-dimensional images were taken every millimeter. All measurements were taken using the rail system Vevo 770 to maintain probe placement and allow for minute adjustments of position. Left ventricular inner diameters during diastole and systole were determined from M-modes along with heart rate. Diastolic and systolic volumes were acquired by applying Simpson's rule of discs to the serially acquired short axis images. Stroke volume was calculated as: diastolic volume − systolic volume. Ejection fraction was calculated as: (stroke volume/diastolic volume) × 100%. Cardiac output was determined by: stroke volume × heart rate.

Masson's Trichrome Staining—After 5 and 28 days (to assess early and late stage heart failure), the infarcted and sham-operated mice were euthanized, and the hearts were rapidly excised and fixed for immunohistochemical analysis or immediately frozen in liquid nitrogen and stored at −80 °C. In brief, after excision, sham and infarcted mouse hearts (5 and 28 days) were fixed in 4% paraformaldehyde for 1 h at 4 °C, then kept in PBS with 30% sucrose overnight at 4 °C, embedded in optimal cutting temperature compound (Sakura Finetek, Torrance, CA), sectioned (10 μm) with cryostat (Leica, Germany), and placed on superfrost slides. The degree of myocardial infarction (MI) was evaluated using Masson's trichrome staining kit according to manufacturer's protocol (Sigma).

miRNA Microarray and Real-time PCR—Total RNA from the 5- and 28-day sham and infarcted mouse hearts ($n = 4$) was isolated using TRIzol reagent (Invitrogen). Rodent miRNA microarray kit (Applied Biosystems) was used according to the manufacturer's protocol. In brief, 1 μg of total RNA was reverse-transcribed with Megaplex RT primers (Megaplex RT Rodent Pool A), followed by a real-time PCR with TaqMan Rodent MicroRNA Array performed on an Applied Biosystems 7900HT System. SDS software version 2.3 and DataAssist version 3.0 (Applied Biosystems) were used to obtain the comparative threshold cycle (C_t) value. U6 small nuclear RNA included in the TaqMan Rodent MicroRNA Array was used as an endogenous control. Quantitative RT-PCR (qRT-PCR) analyses were carried out using TaqMan miRNA assays (Applied Biosystems) according to the manual. Relative expression of miR-539 was calculated using the $\Delta\Delta C_T$ method normalized to the expression of U6 small nuclear RNA (Applied Biosystems). Relative levels of OGA and OGT mRNA were examined with specific primers (OGA: forward, 5′-TGGAAGACCTTGGGTTATGG-3′ and reverse, 5′-TGCTCAGCTTCTTCCACTGA-3′; OGT, forward, 5′-CCTGGGTCGCTTGGAAGA-3′ and reverse, 5′-TGGTTGCGTCTCAATTGCTTT-3′) using Fast SYBR Green (Applied Biosystems) and normalized to levels of 18 S mRNA. All qRT-PCRs were performed in duplicate.

Cell Culture—Neonatal rat cardiomyocytes (NRCMs) were isolated from 1–2-day-old Sprague-Dawley rats according to the protocol described elsewhere (23). The isolated cardiomyocytes were cultured in DMEM containing 10% fetal bovine serum, penicillin/streptomycin, and vitamin B_{12} in the presence of anti-mitotic BrdU (0.1 mM) for 4 days to inhibit fibroblast growth and subsequently grown in the absence of BrdU. HEK293 cells were grown in DMEM containing 10% fetal bovine serum and penicillin/streptomycin. 293FT cells cultured in DMEM Glutamax (Invitrogen) containing 10% fetal bovine serum, penicillin/streptomycin, and Geneticin (Invitrogen) were used for the lentivirus preparation.

Luciferase Reporter Assay—For luciferase assay, we transiently co-transfected (Lipofectamine 2000, Invitrogen) pLenti6/V5-miR-539 or pLenti6/V5-scrambled (250 ng) overexpressing constructs with luciferase reporter plasmid containing wild type OGA-3′UTR (Genecopoeia, Inc.) or miR-539 binding seed mutant OGA-3′UTR (250 ng) in 60–70% confluent HEK293 cells grown in a 12-well plate. *Renilla* reporter plasmid (10 ng) was used as transfection control. At 48 h post-transfection, cells were lysed and assayed for luciferase activity using a dual luciferase assay kit (Promega).

miRNA-539 Construct and Lentivirus Preparation—The precursor miRNA-539 was amplified from mouse genomic DNA using forward (5′-CACGTGTGAGGAGTGGTGAT-3′) and

reverse (5′-CCTTGTGCCCAGGTAAGG-3′) primers containing EcoRI and XhoI restriction sites, respectively. Scrambled sequence amplified from pEZX-MR04 (GeneCopoeia, Inc.) using forward (5′-ACACCCTGTTTATTGATGCTGA-3′) and reverse (5′-CCTGTTATTCTCTGCTAACGCC-3′) primers was used as a control. The amplified precursor miRNA-539 and scrambled control were cloned into pLenti6/V5 plasmid and verified by sequencing. The integrity of miRNA-539 and scrambled control stem loop structure was analyzed using mfold version 2.3. 3 μg of pLenti6/V5-miR-539 was mixed with 9 μg of ViraPower Packaging Mix (Invitrogen) and transfected in 293FT cells using Lipofectamine 2000 transfection reagent according to the manufacturer's instruction. The pseudolentiviral particles released in the medium were concentered using Lenti-X Concentrator (Clontech Laboratories, Inc.) and titrated in NRCMs by qPCR using SV40 forward, 5′-GCTCCCCAGCAGGCAGAAGTATG-3′ and reverse, 5′-TGGGGAGCCTGGGGACTTTCCAC-3′ primers. pLenti6/V5-mCherry was used as a transduction control.

Functional Study of miRNA-539—We examined the effect of miR-539 on OGA and OGT by transducing NRCMs and HEK293 cells with miR-539 lentivirus or scrambled or mCherry control lentiviruses. The cells were maintained in their regular growth medium for 2 days and selected with blasticidine for 5 days. Alternatively, cells were transfected with mirVana^{TM} miR-539 inhibitor or an negative control Oligonucleotides (10 nmol/liter) using Lipofectamine^{TM} RNAiMAX (Invitrogen) after 5 days of lentivirus treatment. Overexpression of miR-539 expression was verified by qRT-PCR using miRNA assay as described above and the loss or gain of OGA expression followed by miR-539 mimic/inhibitor was analyzed by Western blotting.

Western Blotting—The proteins from the hearts and whole cell lysate were separated in 4–12% NuPAGE BisTris gel by electrophoresis, transferred to PVDF membrane, and probed for OGA (1:1000; sc-135093, Santa Cruz Biotechnology, Inc.), OGT (1:2000; O6264, Sigma), *O*-GlcNAc (1:1000; CTD 110.6, Covance; or RL2, Affinity Bioreagents), α-tubulin, or β-actin (1:2000, Sigma) followed by secondary antibody (Santa Cruz Biotechnology, Inc.) using a standard protocol as described earlier (24). Densitometry analysis was performed using non-saturated chemiluminescent membranes exposed and quantified using Fuji LAS-3000 bio-imaging analyzer.

In Situ Hybridization—MicroRNA-539 *in situ* hybridization was performed using the protocol described by Obernosterer *et al.* (25). In brief, frozen sections of sham and infarcted mouse hearts (5 and 28 days) were prepared as mentioned earlier, washed in PBS for 10 min, placed in acetylation solution (98% diethyl pyrocarbonate-treated water, 1.3% triethanolamine, 0.175% HCl, 12% acetic anhydride) for 20 min and digested by Proteinase K (25 μg/ml) for 5 min at room temperature, washed in PBS for 5 min, and prehybridized (50% formamide, 25% 20× SSC, 10% 50× Denhardt's, 1.25% 20 mg/ml of yeast tRNA, 5% 10 mg/ml of salmon sperm DNA, 0.4 g of blocking reagents in 20 ml of solution and 8.75% diethyl pyrocarbonate-treated water) at 50 °C for 4 h. The digoxigenin-labeled mmu-miR-539 LNA probe (Exiqon, Woburn, MA). Probes (1 nM) were denatured with denaturing hybridization solution (50% formamide, 25% 20× saline-sodium citrate (SSC), 10% 50× Denhardt's, 1.25% 20 mg/ml of yeast tRNA, 5% 10 mg/ml of salmon sperm DNA, 0.4 g of blocking reagents in 20 ml of solution, 2.5% of 10% CHAPS, 0.5 of 20% Tween, and 5.75% diethyl pyrocarbonate-treated water) at 95 °C for 5 min, then added to the slides and hybridized at 50 °C for overnight. The slides were washed in 5× SSC for 5 min followed by 0.2× SSC for 60 min at 60 °C. After blocking for 1 h (2% fetal bovine serum), the sections were incubated with anti-digoxigenin antibody (Roche Applied Science; 1:2000) overnight at 4 °C. The bound antibody was detected by AP substrate, nitro blue tetrazolium chloride/5-bromo-4-chloro-3-indolyl phosphate, toluidine salt for color development for 24–48 h at room temperature in the dark, and imaged using a NS-F12 camera mounted on a Nikon Eclipse Ni microscope.

In Vitro Hypoxia-reoxygenation Injury—To determine whether additional insults, such as hypoxia-reoxygenation alter miR-539 levels, NRCMs were subjected to hypoxia-reoxygenation as described (9). In brief, cells were subjected to 3 h hypoxia in Esumi lethal ischemia medium for glucose and nutrient deprivation (containing 117 mmol/liter of NaCl, 12 mmol/liter of KCl, 0.9 mmol/liter of $CaCl_2$, 0.49 mmol/liter of $MgCl_2$, 4 mmol/liter of HEPES, 20 mmol/liter of sodium lactate, and 5.6 mmol/liter of L-glucose; pH 6.2) in a sealed humidified hypoxic chamber (Billups-Rothenberg, Inc.) flushed with 5% CO_2 and 95% N_2, and maintained at 37 °C. After 3 h, the cells were switched to Esumi control medium (containing 137 mmol/liter of NaCl, 3.8 mmol/liter of KCl, 0.9 mmol/liter of $CaCl_2$, 0.49 mmol/liter of $MgCl_2$, 4 mmol/liter of HEPES, and 5.6 mmol/liter of D-glucose, pH 7.4) and allowed to reoxygenate for 3, 6, and 12 h in the modular incubator. Cells grown in the Esumi control medium for the same durations were used as normoxic controls. The expression of miR-539 and OGA protein level was analyzed as described above.

Statistical Analysis—Unpaired Student's *t* test was used for the comparison between two groups. Analysis of variance was performed when comparisons were made among three or more groups along with Scheffe's post hoc analysis. $p < 0.05$ was accepted as statistically significant.

RESULTS

Myocardial Infarction and Cardiac Function—Masson's trichrome staining showed distinct blue collagen fibers and red myocytes in the sham and infarcted mouse hearts (Fig. 1, *A–D*). At 5 days the infarcted heart showed significantly decreased wall thickness with increased collagen deposition, which was greater at 28 days compared with the sham heart (Fig. 1, *B* and *D*). Echocardiography was performed at 5 and 28 days post-MI to demonstrate the severity of cardiac dysfunction. At 5 days after MI, hearts exhibited significant dilation (Fig. 1, *E–H*) and severely depressed cardiac function, as evidenced by significantly decreased stroke volume, ejection fraction, and cardiac output (Fig. 1, *I–L*) when compared with sham-operated mice. Indeed, this defect persisted; echocardiography confirmed dysfunction 28 days after MI (Fig. 1, *E–L*).

miRNA-539 Is Up-regulated in Failing Heart—Global miRNA profiling analysis revealed that several miRNAs are differentially expressed (<0.7- or >2-fold) in 5- and 28-day failing hearts compared with sham heart (Table 1). To identify the miRNAs that target HBP, we performed target prediction anal-

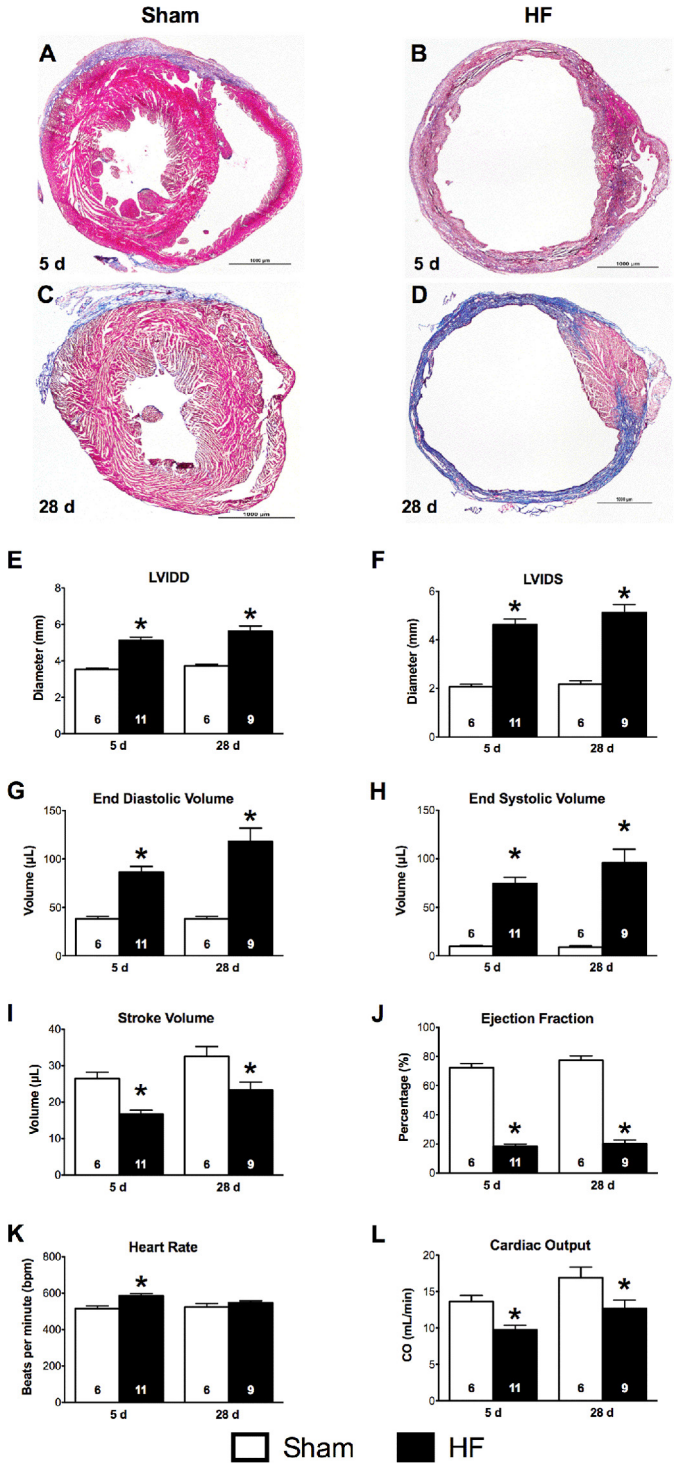

FIGURE 1. **Masson's trichrome staining shows collagen fibers (*blue*) and healthy myocardium (*red*) in sham and infarcted mouse hearts.** *B* and *D* shows a significant decrease in the left ventricular wall thickness with increased collagen deposition and loss of myocardium compared with their respective sham hearts (*A* and *C*). Magnification at ×2; *scale bar* = 1000 μm. MI induced significant left ventricular dysfunction (*E–H*). Mice subjected to MI had severely dilated left ventricles, reduced stroke volume (*I*), and ejection fraction (*J*). Despite elevated heart rates at 5 d following MI (*K*), cardiac output was significantly diminished at both 5 and 28 days (*L*), $p < 0.05$. *LVIDD*, left ventricular internal diameter − diastole; *LVIDS*, left ventricular internal diameter − systole. Group sizes are indicated in the *bars*.

TABLE 1

miRNA expression in the failing heart

The table shows a summary of several miRNAs differentially expressed in 5- and 28-day infarcted mouse heart by miRNA microarray analysis. miR-539 is significantly up-regulated at both 5 and 28 days in the failing hearts compared to sham hearts.

MicroRNA	HF *vs.* sham (mean ± S.D.)	
	5 days	28 days
mmu-let-7g	0.54 ± 0.04	0.48 ± 0.01
mmu-miR-126–5p	0.73 ± 0.05	0.48 ± 0.01
mmu-miR-127	5.89 ± 0.35	3.87 ± 0.01
mmu-miR-128a	0.86 ± 0.15	0.69 ± 0.01
mmu-miR-133a	0.58 ± 0.14	0.48 ± 0.03
mmu-miR-133b	0.52 ± 0.06	0.49 ± 0.01
mmu-miR-135a	0.49 ± 0.04	0.48 ± 0.01
mmu-miR-135b	0.40 ± 0.09	0.24 ± 0.01
mmu-miR-139–5p	0.52 ± 0.04	0.48 ± 0.01
mmu-miR-140	1.77 ± 0.14	1.95 ± 0.01
mmu-miR-142–3p	4.23 ± 1.18	3.24 ± 0.59
mmu-miR-142–5p	3.80 ± 0.25	3.23 ± 0.01
mmu-miR-143	0.64 ± 0.05	0.48 ± 0.01
mmu-miR-145	0.65 ± 0.04	0.48 ± 0.01
mmu-miR-148b	0.70 ± 0.13	0.69 ± 0.02
mmu-miR-150	0.64 ± 0.04	0.49 ± 0.02
mmu-miR-15b	2.36 ± 0.15	1.94 ± 0.01
mmu-miR-181a	1.15 ± 0.11	0.48 ± 0.01
mmu-miR-184	4.88 ± 2.55	4.59 ± 0.96
mmu-miR-187	0.77 ± 0.13	0.48 ± 0.02
mmu-miR-18a	4.24 ± 1.11	2.76 ± 0.02
mmu-miR-194	0.61 ± 0.15	0.48 ± 0.58
mmu-miR-199a-3p	5.23 ± 0.30	3.92 ± 0.01
mmu-miR-200b	0.20 ± 0.15	0.94 ± 0.03
mmu-miR-203	0.56 ± 0.06	0.48 ± 0.01
mmu-miR-204	0.57 ± 0.14	0.49 ± 0.01
mmu-miR-208	0.88 ± 0.39	0.68 ± 0.01
mmu-miR-21	4.59 ± 0.39	3.95 ± 0.01
mmu-miR-214	4.22 ± 1.36	2.75 ± 0.58
mmu-miR-215	0.66 ± 0.04	0.48 ± 0.02
mmu-miR-223	3.17 ± 0.86	1.93 ± 0.02
mmu-miR-224	2.40 ± 0.15	1.93 ± 0.01
mmu-miR-26a	0.61 ± 0.05	0.48 ± 0.04
mmu-miR-296–5p	5.46 ± 0.82	3.92 ± 0.03
mmu-miR-29b	1.07 ± 0.14	0.70 ± 0.58
mmu-miR-30a	0.61 ± 0.04	0.48 ± 0.01
mmu-miR-30b	0.56 ± 0.04	0.49 ± 0.02
mmu-miR-30c	0.52 ± 0.11	0.34 ± 0.58
mmu-miR-30e	0.64 ± 0.12	0.34 ± 0.01
mmu-miR-31	3.19 ± 0.16	1.93 ± 0.01
mmu-miR-328	0.62 ± 0.05	0.48 ± 0.01
mmu-miR-335–3p	2.30 ± 0.18	1.93 ± 0.01
mmu-miR-337–3p	4.31 ± 0.32	3.86 ± 0.01
mmu-miR-337–5p	5.40 ± 0.79	3.89 ± 0.01
mmu-miR-342–3p	1.21 ± 1.38	0.96 ± 0.01
mmu-miR-345–5p	0.62 ± 0.12	0.48 ± 0.01
mmu-miR-34a	0.66 ± 0.05	0.48 ± 0.02
mmu-miR-34b-3p	1.68 ± 0.16	1.94 ± 0.01
mmu-miR-351	2.91 ± 0.17	1.94 ± 0.03
mmu-miR-361	0.88 ± 0.05	0.48 ± 0.01
mmu-miR-362–3p	2.49 ± 0.67	1.36 ± 0.58
mmu-miR-376a	13.82 ± 1.95	6.51 ± 0.02
mmu-miR-376b	3.45 ± 1.56	3.86 ± 0.03
mmu-miR-376c	4.34 ± 0.28	3.89 ± 0.01
mmu-miR-382	4.47 ± 0.48	7.96 ± 0.01
mmu-miR-384–5p	0.60 ± 0.17	0.34 ± 0.02
mmu-miR-409–3p	7.78 ± 3.22	7.71 ± 0.58
mmu-miR-410	6.91 ± 0.36	3.92 ± 0.01
mmu-miR-411	4.62 ± 1.30	3.88 ± 0.01
mmu-miR-434–3p	4.00 ± 1.12	2.70 ± 0.58
mmu-miR-434–5p	3.35 ± 0.99	2.73 ± 0.01
mmu-miR-486	0.46 ± 0.04	0.49 ± 0.01
mmu-miR-487b	4.05 ± 1.04	2.73 ± 0.58
mmu-miR-495	3.96 ± 0.23	3.93 ± 0.01
mmu-miR-499	0.55 ± 0.04	0.48 ± 0.01
mmu-miR-500	2.82 ± 0.73	2.77 ± 0.01
mmu-miR-503	3.54 ± 0.33	3.85 ± 0.01
mmu-miR-539	6.98 ± 2.82	5.59 ± 0.01
mmu-miR-542–5p	0.66 ± 0.04	0.48 ± 0.03
mmu-miR-543	1.79 ± 0.16	1.94 ± 0.01
mmu-miR-652	1.71 ± 0.14	1.95 ± 0.01
mmu-miR-667	4.73 ± 0.27	3.82 ± 0.01
mmu-miR-674	2.18 ± 0.60	1.93 ± 0.58
mmu-miR-685	1.52 ± 0.42	1.93 ± 0.02
mmu-miR-7a	2.64 ± 0.81	1.94 ± 0.01

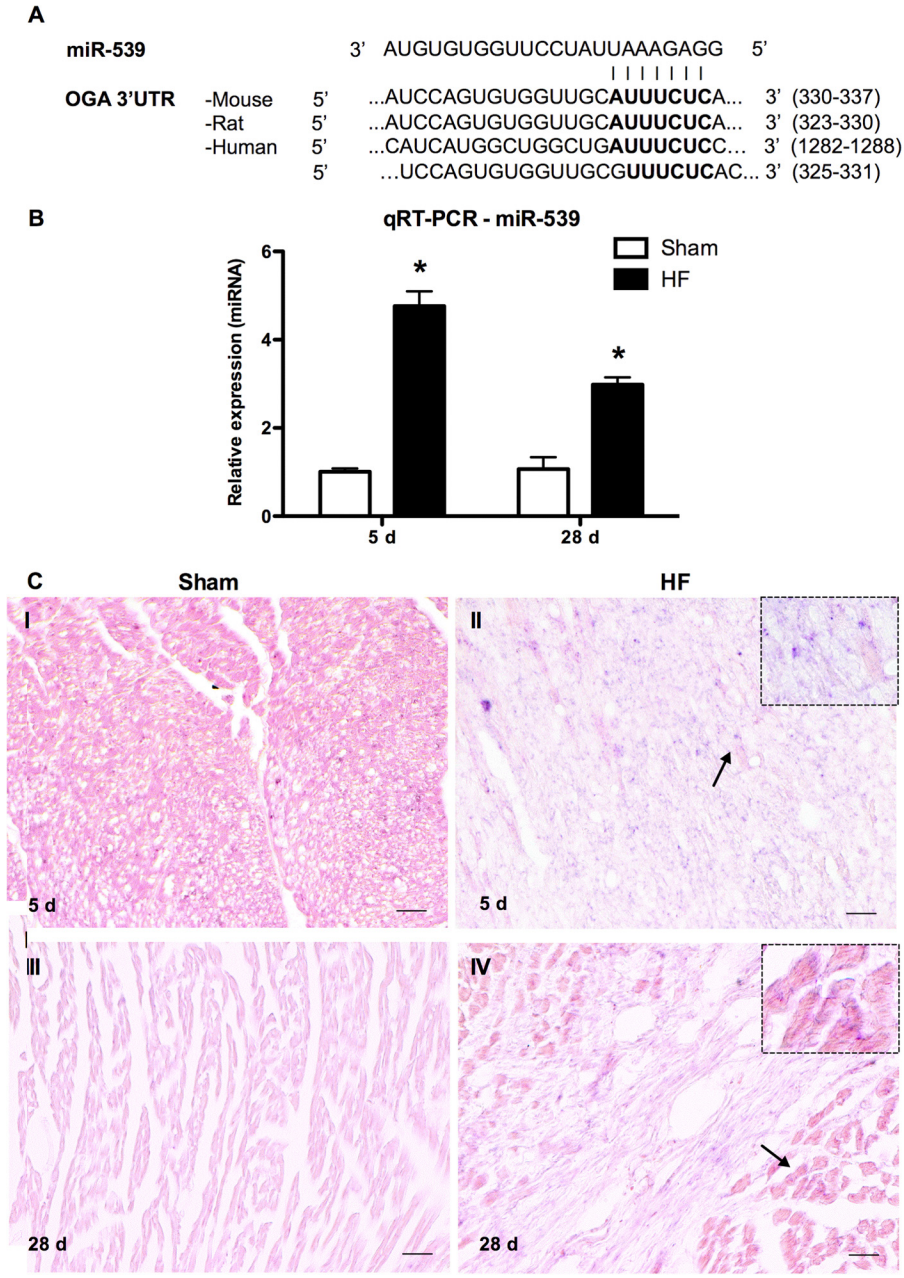

FIGURE 2. **Up-regulation of miR-539 in the failing heart.** *A,* miRNA-539 binding sites in the OGA-3′UTR are conserved among mouse, rat, and human. TargetScan 6.2, where human OGA-3′UTR has two putative miR-539 binding sites. *B,* expression of miR-539 was measured by qRT-PCR and normalized to the expression of U6 in each sample. The failing heart shows significant up-regulation of miR-539 in 5 ($p < 0.001$) and 28 day ($p < 0.05$) compared with sham heart. *C,* probing of miR-539 LNA in the cryosections using *in situ* hybridization shows increased miR-539 expression (in *purple*) in the remote zone of the failing heart (*II* and *IV*) compared with the sham heart (*I* and *III*). Histological observation also reveals perinuclear localization of miR-539 in the cardiomyocytes (*insets*). Low magnification images were taken at ×20; *insets* are at ×60 magnification. *Scale bar* = 10 μm.

ysis (TargetScan and MiRanda algorithms) and found a predicted miR-539 binding site in OGA-3′UTR (26). The miR-539 binding sites in the OGA-3′UTR are conserved among mouse, rat, and human (Fig. 2*A*). We performed qRT-PCR to confirm the miRNA microarray data. Specifically, miRNA-539 was up-regulated ~5- and ~3-fold ($p < 0.05$) in 5 and 28 days, respectively, in the infarcted heart compared with sham heart (Fig. 2*B*). Further *in situ* hybridization analysis with the miR-539 LNA probe revealed increased expression of miR-539 in the remote zone (non-infarcted) of the failing heart compared with the sham heart (Fig. 2*C*). Interestingly, a strong signal of miR-539 was observed in 5-day compared with 28-day failing heart and the sham hearts showed weak signals at both 5 and 28 days. Histomorphological observation also showed the perinuclear localization of miR-539 in the cardiomyocytes. Collectively these data demonstrate that miR-539 was significantly up-regulated in the failing heart by 5 days and through at least 28 days.

Reduced OGA Expression and Increased O-GlcNAcylation in the Failing Heart—Use of qRT-PCR analysis showed significant down-regulation of OGA mRNA and protein levels in both 5- and 28-day infarcted hearts compared with sham hearts (Fig. 3, *A* and *B*). A significant increase in OGT mRNA expression was observed

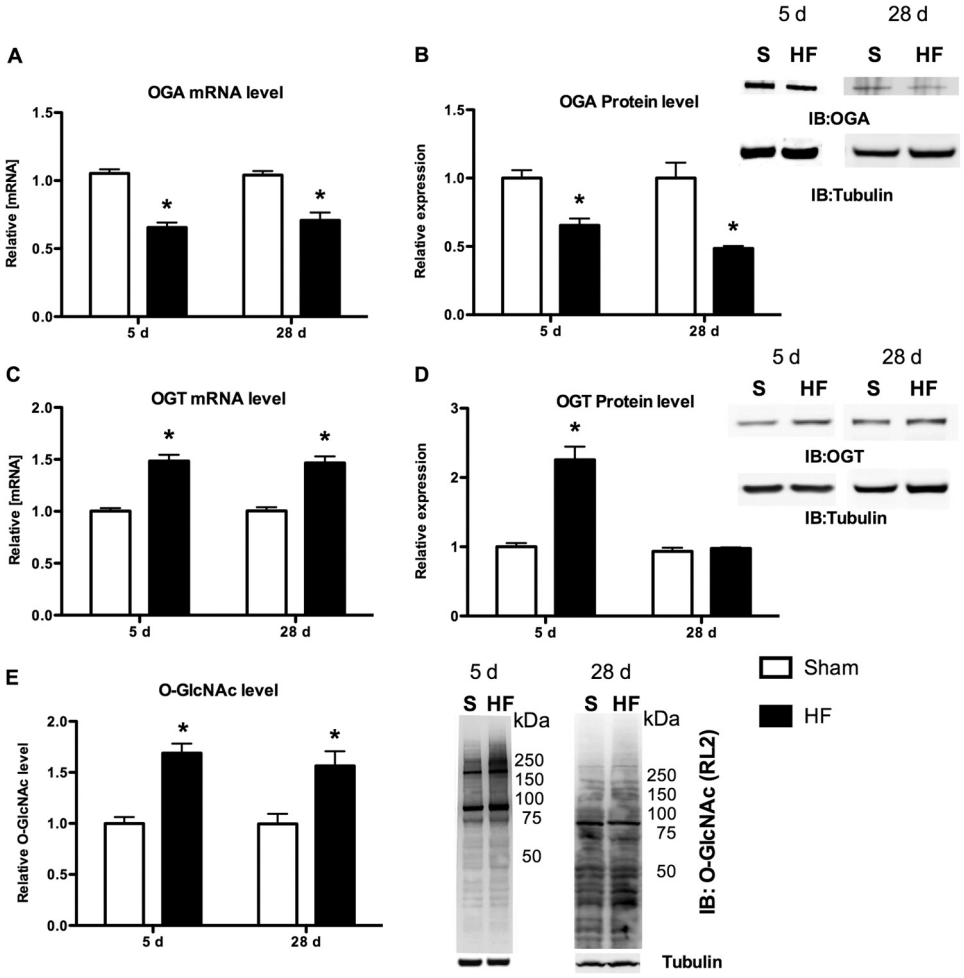

FIGURE 3. **Down-regulation of OGA expression and increased protein *O*-GlcNAcylation in the failing heart.** *A*, OGA expression was measured by qRT-PCR and normalized to the expression of 18 S rRNA, which shows significant down-regulation in the failing heart compared with the sham heart at 5 and 28 days; $p < 0.0001$. *B*, Western blot analysis from the 5- and 28-day failing heart shows significant down-regulation of OGA at the protein level ($p < 0.01$). *C*, qRT-PCR analysis shows significant up-regulation of OGT in the failing heart compared with sham heart at 5 and 28 days; $p < 0.0001$. *D*, Western blot analysis shows and increased OGT protein level in 5-day failing heart ($p < 0.0001$) but not at 28 days. *E*, significant increase in protein *O*-GlcNAcylation compared with sham heart; $p < 0.001$. Data are expressed as the mean ± S.E. ($n = 4$/group). *IB*, immunoblot.

in 5- and 28-day infarcted hearts, which was accompanied by a significant increase in OGT protein at 5 days, but not 28 days (Fig. 3, *C* and *D*). In addition, there was a significant increase in protein *O*-GlcNAcylation at both 5 and 28 days in infarcted hearts (Fig. 3*E*).

miRNA-539 Targets OGA-3′UTR—To test whether miR-539 binds directly to the OGA-3′UTR as predicted, we co-transfected reporter plasmid containing luciferase upstream to the OGA-3′UTR or miR-539 binding site mutant (Fig. 4*A*) with scrambled control or miRNA-539 expression plasmids in HEK293 cells. Co-transfection of wild-type OGA-3′UTR with miR-539 significantly reduced luciferase activity (>40%) compared with scrambled control. In contrast, co-transfection of the miR-539 binding site mutant with miR-539 did not affect the luciferase activity (Fig. 4*B*). These results suggest that miR-539 binds to the OGA-3′UTR, thereby providing a potential mechanism to reduce OGA expression.

miRNA-539 Modulates OGA Expression in Vitro—To determine whether overexpression of miR-539 suppresses OGA expression, we transduced NRCMs and HEK293 cells with miR-539 lentivirus to overexpress miR-539. Real-time PCR analysis showed significant up-regulation of miR-539 in both NRCMs (~170-fold) and HEK293 cells (~35,000-fold) transduced with miR-539 lentivirus compared with scrambled virus (Fig. 4, *C* and *E*). Immunoblot analysis showed ~40% reduction in OGA expression in miR-539 overexpressed NRCMs compared with scrambled control or mCherry-transduced NRCMs (Fig. 4*D*), whereas HEK293 showed ~30% reduction in OGA expression in miR-539 overexpressed cells compared with scrambled control (Fig. 4*F*). Furthermore, transfection with the miR-539 inhibitor rescued OGA protein expression in miR-539 overexpressing NRCMs (Fig. 5, *A* and *B*) and HEK293 cells (Fig. 6, *A* and *B*) compared with negative control inhibitor-treated cells. Such findings indicate that overexpression of miR-539 significantly suppresses OGA expression in NRCMs. Interestingly, we found the OGT protein levels were also significantly diminished following miR-539 overexpression in this *in vitro* system (Figs. 5, *C* and *D*, and 6, *C* and *D*).

Effect of miRNA-539 on O-GlcNAcylation—To assess the functional consequence of miR-539-mediated OGA regulation, miR-539 overexpressed or expression-silenced NRCMs and HEK293 cells were assessed for *O*-GlcNAc levels. Overexpres-

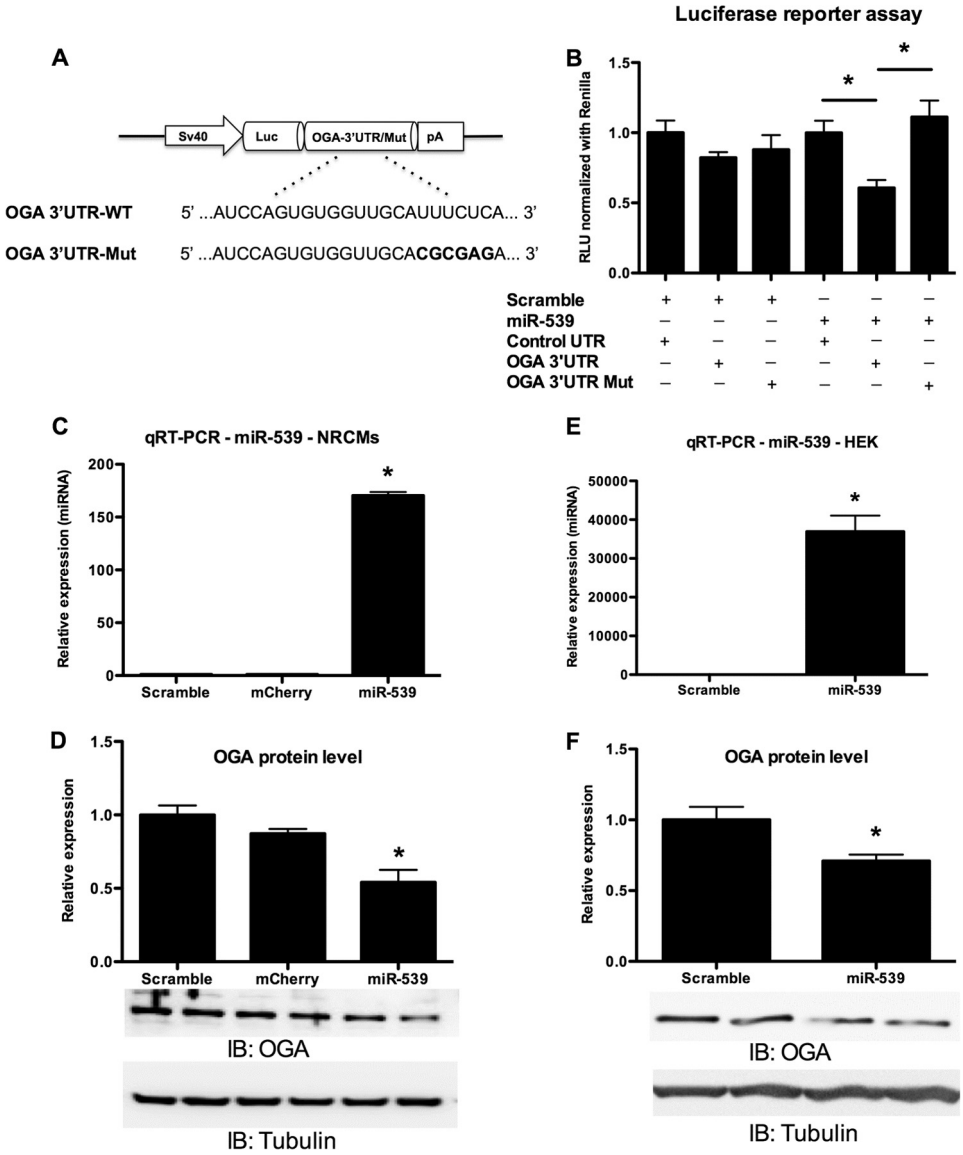

FIGURE 4. **miR-539 regulates OGA expression.** *A*, reporter plasmid containing luciferase upstream to the OGA-3′UTR was obtained from Genecopoeia and the miR-539 binding site seed sequence (AUUUCUC) was mutated (ACGCGAG) by site-directed mutagenesis using mutated forward and reverse primers. *B*, luciferase activity was measured after 48 h from HEK293 lysates co-transfected with OGA-3′UTR or miR-539 binding site mutant with scrambled or miRNA-539 expression plasmids. Luciferase activity was normalized with internal *Renilla* control. Significant down-regulation of luciferase activity was determined by miR-539 when co-transfected with OGA-3′UTR, whereas the miR-539 binding site mutation was unaffected; $p < 0.05$. *C* and *E*, qPCR analysis a shows significant level of miR-539 expression in NRCMs and HEK293 cells transduced with lentivirus encoding miR-539 ($n = 3$/group) compared with mCherry-transduced cells; $p < 0.0001$. *D* and *F*, Western blot analysis and respective quantitative analysis shows around 40 ($p < 0.005$) and 30% ($p < 0.05$) reduction of OGA expression in miR-539 overexpressing NRCMs and HEK293 cells, respectively, compared with scrambled controls ($n = 3$/group). *IB*, immunoblot.

sion of miR-539 significantly increased *O*-GlcNAc levels, whereas inhibition of miR-539 in miR-539 stably expressing NRCMs and HEK293 cells reduced *O*-GlcNAc to normal levels (Figs. 5, *E* and *F,* and 6, *E* and *F*).

Hypoxia-reoxygenation Increases miR-539 and Decreases OGA Expression—To determine whether miR-539 might play a role in regulating OGA expression in an *in vitro* proxy for a pathologic condition, we subjected NRCMs to hypoxia-reoxygenation. Indeed, the level of miR-539 was significantly increased after 3 h of reoxygenation with a decrease in the OGA protein level after 6 and 12 h of reoxygenation (Fig. 7, *A* and *B*). Thus, miR-539 is up-regulated in NRCMs following hypoxia, and is associated with a reduction in OGA expression.

DISCUSSION

More than 1,000 nuclear and cytoplasmic proteins are known to be *O*-GlcNAcylated, including targets important for transcription, translation, signal transduction, and cell cycle control (27–30). In response to various stresses, global augmentation of protein *O*-GlcNAcylation confers a survival advantage at the cellular level. Several *in vitro* and *in vivo* analyses showed *O*-GlcNAc-mediated cardioprotection against ischemia-reperfusion, myocardial infarction, and oxidative stress (4, 7, 9, 31–33). The present study indicates that down-regulation of OGA may be involved, at least partially, in increased *O*-GlcNAcylation in non-reperfused myocardial infarction.

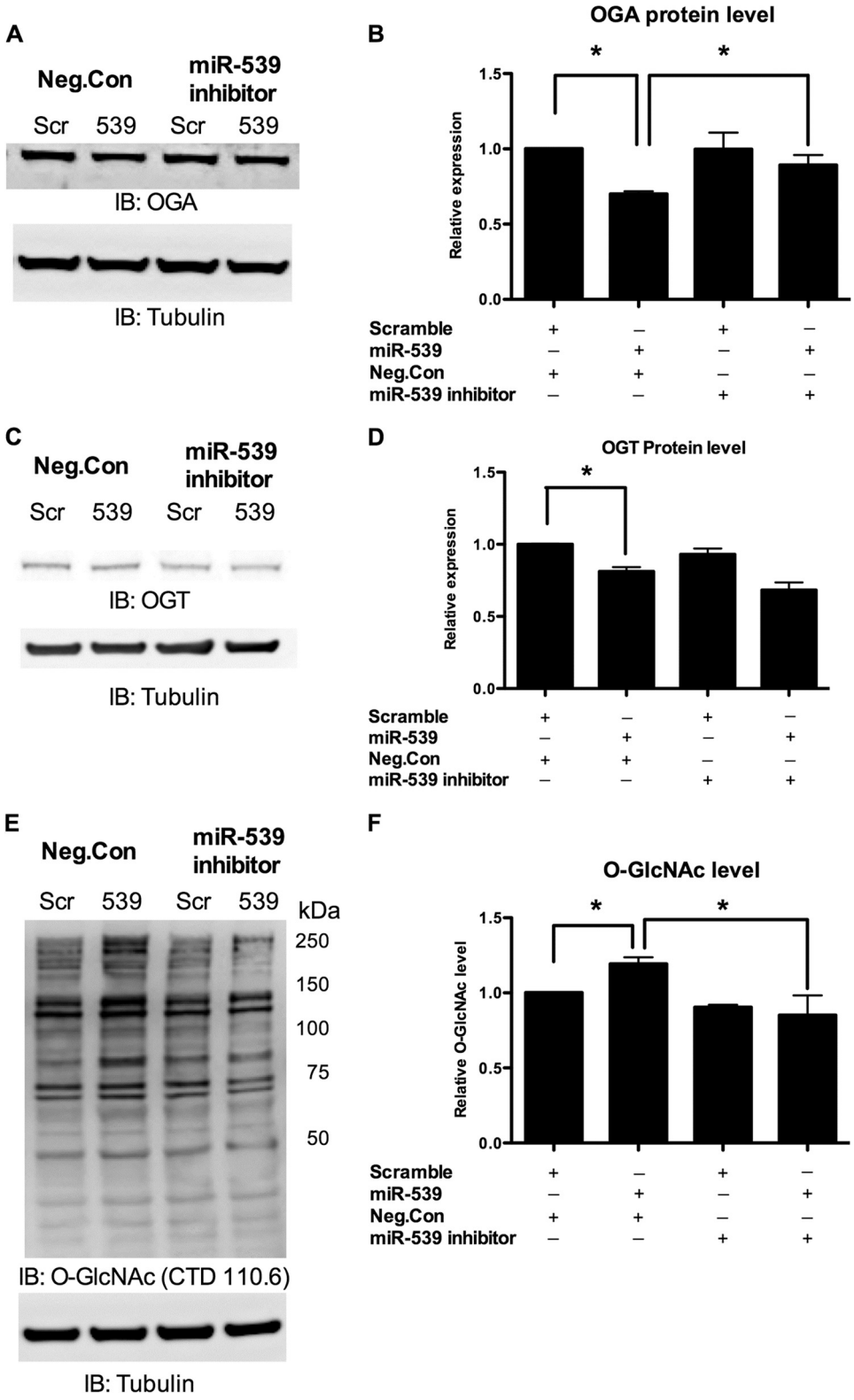

FIGURE 5. **Inhibition of miR-539 rescues OGA expression and *O*-GlcNAcylation in NRCMs.** *A–D*, Western blot analysis shows a significant reduction of OGA and OGT levels transduced with miRNA-539 upon negative control treatment, whereas anti-miR-539 transfection rescued the OGA expression toward the normal level ($n = 3$/group); $p < 0.05$. *E* and *F*, Western blot analysis shows a significant increase in protein *O*-GlcNAcylation by miR-539 overexpression, and inhibition of miR-539 brought *the O*-GlcNAc level to normal ($n = 3$/group); $p < 0.05$. *IB*, immunoblot.

Numerous gain- and loss-of-function studies have uncovered prominent roles for miRNAs in human cardiovascular disorders including myocardial infarction, cardiac hypertrophy, heart failure, fibrosis, and pressure overload-induced remodeling (34–38). Few studies focused on miRNAs implicated in metabolic disorders (39, 40), yet, there are no prior studies

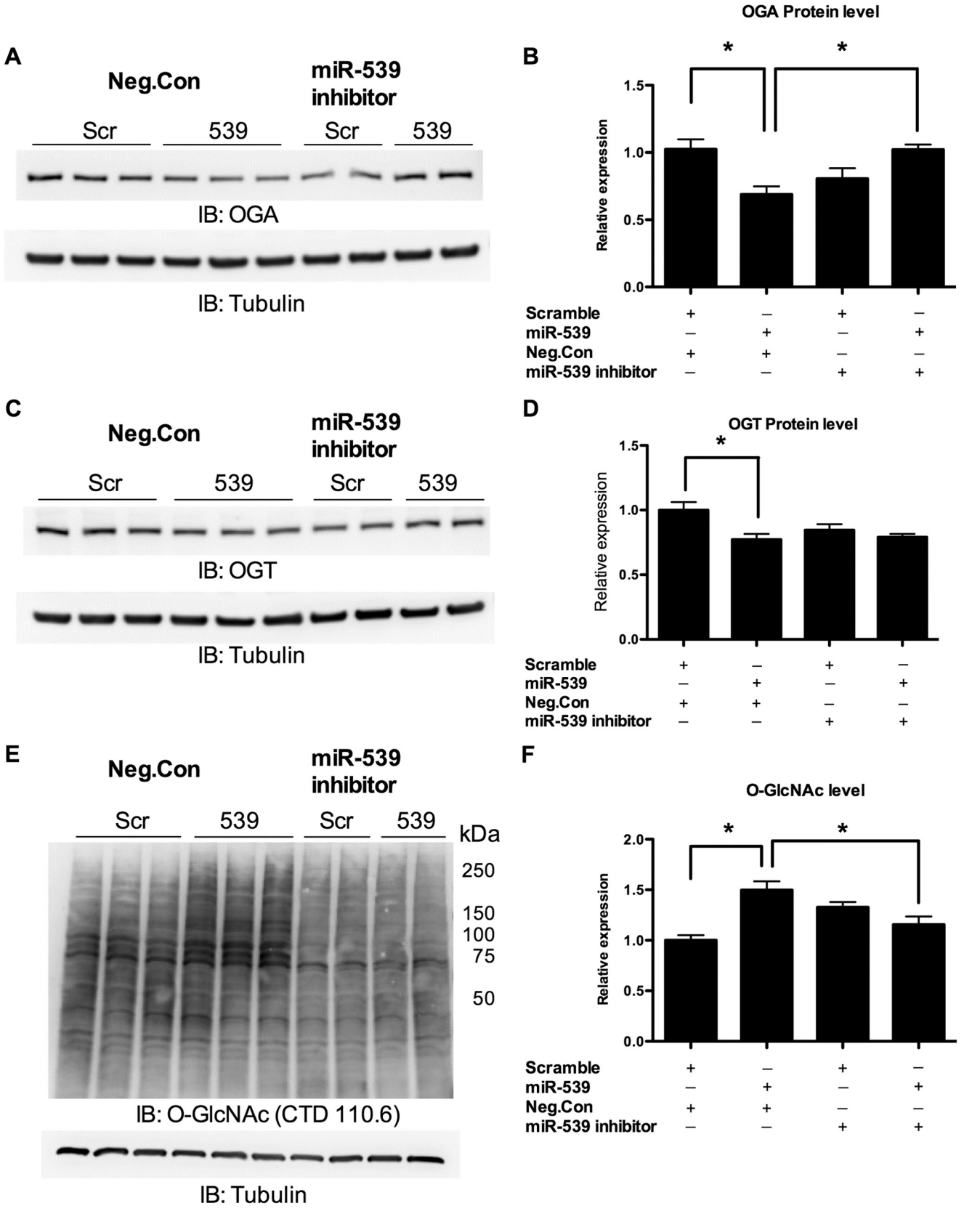

FIGURE 6. **Negative regulatory effect of miR-539 on OGA expression in human, non-cardiac cell types.** *A–D,* Western blot analysis shows a significant reduction of OGA and OGT levels in HEK293 cells transduced with miR-539; anti-miR-539 transfection rescued OGA expression toward the basal level ($n = 3$/group); $p < 0.05$. *E* and *F,* Western blot analysis shows a significant increase in protein *O*-GlcNAcylation by miR-539 overexpression, and inhibition of miR-539 returned *O*-GlcNAc levels to normal ($n = 3$/group); $p < 0.001$. *IB*, immunoblot.

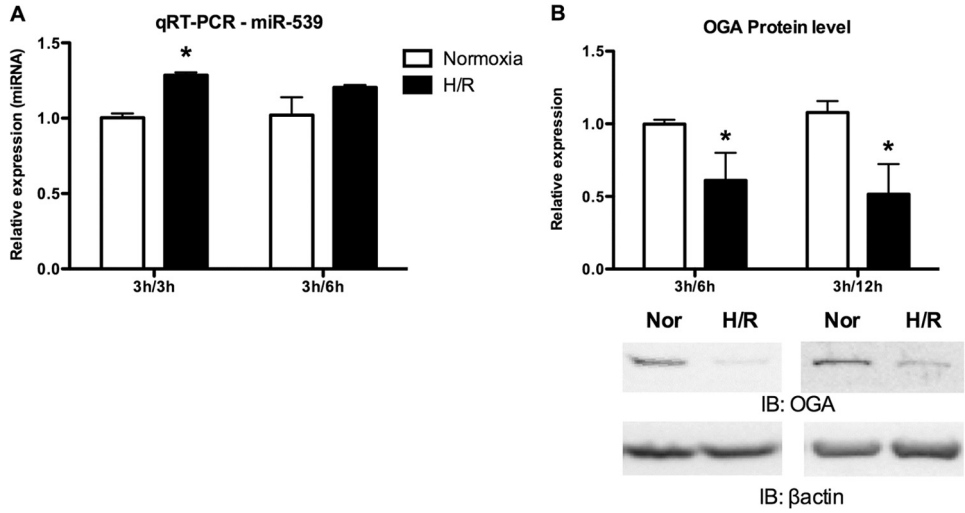

FIGURE 7. **Hypoxia-reoxygenation induces miR-539 expression followed by a decrease in OGA expression.** NRCMs subjected to 3 h of hypoxia were reoxygenated for 3, 6, and 12 h. qRT-PCR analysis shows a significant increase in miR-539 expression at 3 h reoxygenation; $p < 0.05$. Western blot analysis shows a significant decrease in OGA protein level at both 6 and 12 h of reoxygenation ($n = 4$/group); $p < 0.001$. *IB*, immunoblot.

demonstrating miRNA-mediated regulation of OGA (or OGT) expression. In this study, we report a novel paradigm of miRNA-mediated down-regulation of OGA with subsequent augmentation of *O*-GlcNAcylation in the failing heart. Use of miRNA microarray followed by qRT-PCR analysis clearly demonstrated that miR-539 was up-regulated in the failing heart.

Significant down-regulation of OGA in miR-539 overexpressing NRCM (rat) and HEK293 (human) cells indicates that OGA is a potential conserved target of miR-539. Although OGT does not have target sites for miR-539 binding, reduction of the OGT protein level by miR-539 overexpression reveals that there could be indirect mechanisms involved in the regulation of OGT by OGA or other targets of miR-539. Increased OGA expression with concomitant reduction in *O*-GlcNAcylation using the miR-539 inhibitor in both NRCMs and HEK293 cells overexpressing miR-539 indicates that miR-539 may be a potential marker/target of disease or other prognostic indicator.

MicroRNA-539 is present in the miRNA-rich intragenic region of mouse chromosome 12 (NC_000078.6 (109728129 to 109728202)) between *Rian* (RNA imprinted and accumulated in nucleus) and *Mirg* (miRNA containing gene). There are few reports of verified targets of miR-539. Recently, Milosevic *et al.* (41) observed TGF-β1-mediated stimulation of the cluster of microRNAs from chr14q32 (mouse analog; chr12qF1) in normal human lung fibroblasts where miR-539 is one among them; however, the exact mechanism of miR-539 expression *per se* requires further investigation. Interestingly, a recent study indicates that miR-539 regulates mitochondrial fission and apoptosis by targeting prohibitin 2 (PHB2) in cardiomyocytes (42). It is possible that miR-539 plays an even larger role than simply regulating OGA expression. In mast cells, CD117 (*i.e.* KIT or c-kit) represses miR-539 expression, thereby de-repressing microphthalmia-associated transcription factor expression and promoting proliferation (43). In other cell types, miR-539 expression may be biotin-sensitive, and miR-539 targets the mRNA of holocarboxylase synthase, which participates in genetic stability (44). Such collective findings create interesting implications for a more detailed understanding of the molecular interactions governing *O*-GlcNAc-dependent cell function; however, there is no evidence, at present to directly link the aforementioned observations to one another, at least at the level of *O*-GlcNAcylation.

It is also tempting to speculate whether miR-539 plays a role in other cardiovascular diseases in which *O*-GlcNAc appears to be involved. For example, during hypertension, inhibition of OGA increases arterial vascular reactivity (45). Another study demonstrated that OGA inhibition improved cardiac function during reperfusion (46). Our results demonstrate that up-regulation of miR-539 might be a possible molecular mechanism that suppresses OGA expression in the infarcted, failing heart, which, in turn favors *O*-GlcNAcylation. The increase in miR-539 followed by a decrease in OGA protein level during hypoxia-reoxygenation mimics the phenomenon seen in the present *in vivo* myocardial infarction data. Future studies will directly interrogate the role of miR-539 in the evolution of disease and subsequent recovery.

Understanding the regulation of *O*-GlcNAcylation holds critical importance not only in heart failure but also in multiple diseases; no disease exemplifies the potential impact better than diabetes. Several studies suggest that elevated *O*-GlcNAc levels contribute to diabetic cardiomyopathy (47). In humans, the OGA/MGEA5 chromosome locus 10q24.1 is associated with late-onset Alzheimer disease (48). Experimental observations demonstrated that inhibition of OGA decreases phosphorylation of Tau and protects against Tau-mediated neurodegeneration as well as prevents amyloid-β load by increasing the amount of secreted amyloid precursor protein (sAPPα) (49, 50). This line of evidences suggests that increased *O*-GlcNAcylation by OGA inhibition improves neuronal outcome.

In addition, numerous studies showed hyper *O*-GlcNAcylation, increased expression of OGT, and decreased OGA expression in various cancers (51, 52). In part, hyper *O*-GlcNAcylation was also observed as a mechanism that promotes cancer cell survival and stress resistance. Similar to the approach of targeting

kinases, targeting OGA and OGT could be a valuable approach in many cancer therapies. Thus, the implications for our findings with miR-539 could be broad and manifold.

In light of results from this study, it will be interesting to see whether miR-539 expression is altered in these diseases and the use of miR-539 mimic or inhibitor may contribute a new and broad therapeutic approach to modulate *O*-GlcNAc signaling. Moreover, it is time to more carefully investigate the transcriptional and post-transcriptional regulation of OGT and OGA in relevant disease models.

Acknowledgments—We are grateful for the expert technical assistance of Bethany W. Long and Linda T. Harrison. Lakshmanan Annamalai, DVM, PhD (Director, Pathology Core) provided expert insight with the in situ hybridization.

REFERENCES

1. Mudd, J. O., and Kass, D. A. (2008) Tackling heart failure in the twenty-first century. *Nature* **451,** 919–928
2. Ngoh, G. A., and Jones, S. P. (2008) New insights into metabolic signaling and cell survival: the role of β-*O*-linkage of *N*-acetylglucosamine. *J. Pharmacol. Exp. Ther.* **327,** 602–609
3. Zachara, N. E., and Hart, G. W. (2006) Cell signaling, the essential role of *O*-GlcNAc!. *Biochim. Biophys. Acta* **1761,** 599–617
4. Jones, S. P., Zachara, N. E., Ngoh, G. A., Hill, B. G., Teshima, Y., Bhatnagar, A., Hart, G. W., and Marbán, E. (2008) Cardioprotection by *N*-acetylglucosamine linkage to cellular proteins. *Circulation* **117,** 1172–1182
5. Laczy, B. (2009) Protein *O*-GlcNAcylation: a new signaling paradigm for the cardiovascular system. *Am. J. Physiol. Heart Circ. Physiol.* **296,** H13–H28
6. Hart, G. W., Slawson, C., Ramirez-Correa, G., and Lagerlof, O. (2011) Cross talk between *O*-GlcNAcylation and phosphorylation: roles in signaling, transcription, and chronic disease. *Annu. Rev. Biochem.* **80,** 825–858
7. Zachara, N. E., O'Donnell, N., Cheung, W. D., Mercer, J. J., Marth, J. D., and Hart, G. W. (2004) Dynamic *O*-GlcNAc modification of nucleocytoplasmic proteins in response to stress. A survival response of mammalian cells. *J. Biol. Chem.* **279,** 30133–30142
8. Champattanachai, V., Marchase, R. B., and Chatham, J. C. (2007) Glucosamine protects neonatal cardiomyocytes from ischemia-reperfusion injury via increased proteinassociated *O*-GlcNAc. *Am. J. Physiol. Cell Physiol.* **292,** C178–C187
9. Zafir, A., Readnower, R., Long, B. W., McCracken, J., Aird, A., Alvarez, A., Cummins, T. D., Li, Q., Hill, B. G., Bhatnagar, A., Prabhu, S. D., Bolli, R., and Jones, S. P. (2013) Protein *O*-GlcNAcylation is a novel cytoprotective signal in cardiac stem cells. *Stem Cells* **31,** 765–775
10. Ngoh, G. A., Facundo, H. T., Zafir, A., and Jones, S. P. (2010) *O*-GlcNAc signaling in the cardiovascular system. *Circ. Res.* **107,** 171–185
11. Watson, L. J., Facundo, H. T., Ngoh, G. A., Ameen, M., Brainard, R. E., Lemma, K. M., Long, B. W., Prabhu, S. D., Xuan, Y. T., and Jones, S. P. (2010) *O*-Linked β-*N*-acetylglucosamine transferase is indispensable in the failing heart. *Proc. Natl. Acad. Sci. U.S.A.* **107,** 17797–17802
12. Small, E. M., and Olson, E. N. (2011) Pervasive roles of microRNAs in cardiovascular biology. *Nature* **469,** 336–342
13. D'Alessandra, Y., Devanna, P., Limana, F., Straino, S., Di Carlo, A., Brambilla, P. G., Rubino, M., Carena, M. C., Spazzafumo, L., De Simone, M., Micheli, B., Biglioli, P., Achilli, F., Martelli, F., Maggiolini, S., Marenzi, G., Pompilio, G., and Capogrossi, M. C. (2010) Circulating microRNAs are new and sensitive biomarkers of myocardial infarction. *Eur. Heart J.* **31,** 2765–2773
14. Divakaran, V., and Mann, D. L. (2008) The emerging role of microRNAs in cardiac remodeling and heart failure. *Circ. Res.* **103,** 1072–1083
15. Dong, S., Cheng, Y., Yang, J., Li, J., Liu, X., Wang, X., Wang, D., Krall, T. J., Delphin, E. S., and Zhang, C. (2009) MicroRNA expression signature and the role of microRNA-21 in the early phase of acute myocardial infarction. *J. Biol. Chem.* **284,** 29514–29525
16. Brainard, R. E., Watson, L. J., Demartino, A. M., Brittian, K. R., Readnower, R. D., Boakye, A. A., Zhang, D., Hoetker, J. D., Bhatnagar, A., Baba, S. P., and Jones, S. P. (2013) High fat feeding in mice is insufficient to induce cardiac dysfunction and does not exacerbate heart failure. *PloS One* **8,** e83174
17. Jones, S. P., Greer, J. J., van Haperen, R., Duncker, D. J., de Crom, R., and Lefer, D. J. (2003) Endothelial nitric oxide synthase overexpression attenuates congestive heart failure in mice. *Proc. Natl. Acad. Sci. U.S.A.* **100,** 4891–4896
18. Jones, S. P., and Lefer, D. J. (2001) Cardioprotective actions of acute HMG-CoA reductase inhibition in the setting of myocardial infarction. *Acta Physiol. Scand.* **173,** 139–143
19. Greer, J. J., Kakkar, A. K., Elrod, J. W., Watson, L. J., Jones, S. P., and Lefer, D. J. (2006) Low-dose simvastatin improves survival and ventricular function via eNOS in congestive heart failure. *Am. J. Physiol. Heart Circ. Physiol.* **291,** H2743–H2751
20. Jones, S. P., Greer, J. J., Ware, P. D., Yang, J., Walsh, K., and Lefer, D. J. (2005) Deficiency of iNOS does not attenuate severe congestive heart failure in mice. *Am. J. Physiol. Heart Circ. Physiol.* **288,** H365–H370
21. Watson, L. J., Long, B. W., DeMartino, A. M., Brittian, K. R., Readnower, R. D., Brainard, R. E., Cummins, T. D., Annamalai, L., Hill, B. G., and Jones, S. P. (2014) Cardiomyocyte Ogt is essential for postnatal viability. *Am. J. Physiol. Heart Circ. Physiol.* **306,** H142–H153
22. Sansbury, B. E., DeMartino, A. M., Xie, Z., Brooks, A. C., Brainard, R. E., Watson, L. J., DeFilippis, A. P., Cummins, T. D., Harbeson, M. A., Brittian, K. R., Prabhu, S. D., Bhatnagar, A., Jones, S. P., and Hill, B. G. (2014) Metabolomic analysis of pressure-overloaded and infarcted mouse hearts. *Circulation* **7,** 634–642
23. Jones, S. P., Teshima, Y., Akao, M., and Marbán, E. (2003) Simvastatin attenuates oxidant-induced mitochondrial dysfunction in cardiac myocytes. *Circ. Res.* **93,** 697–699
24. Facundo, H. T., Brainard, R. E., Watson, L. J., Ngoh, G. A., Hamid, T., Prabhu, S. D., and Jones, S. P. (2012) *O*-GlcNAc signaling is essential for NFAT-mediated transcriptional reprogramming during cardiomyocyte hypertrophy. *Am. J. Physiol. Heart Circ. Physiol.* **302,** H2122–H2130
25. Obernosterer, G., Martinez, J., and Alenius, M. (2007) Locked nucleic acid-based *in situ* detection of microRNAs in mouse tissue sections. *Nat. Protoc.* **2,** 1508–1514
26. Lewis, B. P., Burge, C. B., and Bartel, D. P. (2005) Conserved seed pairing, often flanked by adenosines, indicates that thousands of human genes are microRNA targets. *Cell* **120,** 15–20
27. Ozcan, S., Andrali, S. S., and Cantrell, J. E. (2010) Modulation of transcription factor function by *O*-GlcNAc modification. *Biochim. Biophys. Acta* **1799,** 353–364
28. Hart, G. W., Housley, M. P., and Slawson, C. (2007) Cycling of *O*-linked β-*N*-acetylglucosamine on nucleocytoplasmic proteins. *Nature* **446,** 1017–1022
29. Housley, M. P., Rodgers, J. T., Udeshi, N. D., Kelly, T. J., Shabanowitz, J., Hunt, D. F., Puigserver, P., and Hart, G. W. (2008) *O*-GlcNAc regulates FoxO activation in response to glucose. *J. Biol. Chem.* **283,** 16283–16292
30. Slawson, C., Zachara, N. E., Vosseller, K., Cheung, W. D., Lane, M. D., and Hart, G. W. (2005) Perturbations in *O*-linked β-*N*-acetylglucosamine protein modification cause severe defects in mitotic progression and cytokinesis. *J. Biol. Chem.* **280,** 32944–32956
31. Groves, J. A., Lee, A., Yildirir, G., and Zachara, N. E. (2013) Dynamic *O*-GlcNAcylation and its roles in the cellular stress response and homeostasis. *Cell Stress Chaperones* **18,** 535–558
32. Ngoh, G. A., Hamid, T., Prabhu, S. D., and Jones, S. P. (2009) *O*-GlcNAc signaling attenuates ER stress-induced cardiomyocyte death. *Am. J. Physiol. Heart Circ. Physiol.* **297,** H1711–H1719
33. Ngoh, G. A., Watson, L. J., Facundo, H. T., and Jones, S. P. (2011) Augmented *O*-GlcNAc signaling attenuates oxidative stress and calcium overload in cardiomyocytes. *Amino Acids* **40,** 895–911
34. Thum, T., Gross, C., Fiedler, J., Fischer, T., Kissler, S., Bussen, M., Galuppo, P., Just, S., Rottbauer, W., Frantz, S., Castoldi, M., Soutschek, J., Koteliansky, V., Rosenwald, A., Basson, M. A., Licht, J. D., Pena, J. T.,

Rouhanifard, S. H., Muckenthaler, M. U., Tuschl, T., Martin, G. R., Bauersachs, J., and Engelhardt, S. (2008) MicroRNA-21 contributes to myocardial disease by stimulating MAP kinase signalling in fibroblasts. *Nature* **456,** 980–984

35. van Rooij, E., Sutherland, L. B., Thatcher, J. E., DiMaio, J. M., Naseem, R. H., Marshall, W. S., Hill, J. A., and Olson, E. N. (2008) Dysregulation of microRNAs after myocardial infarction reveals a role of miR-29 in cardiac fibrosis. *Proc. Natl. Acad. Sci. U.S.A.* **105,** 13027–13032
36. Callis, T. E., Pandya, K., Seok, H. Y., Tang, R. H., Tatsuguchi, M., Huang, Z. P., Chen, J. F., Deng, Z., Gunn, B., Shumate, J., Willis, M. S., Selzman, C. H., and Wang, D. Z. (2009) MicroRNA-208a is a regulator of cardiac hypertrophy and conduction in mice. *J. Clin. Invest.* **119,** 2772–2786
37. van Rooij, E., Sutherland, L. B., Qi, X., Richardson, J. A., Hill, J., and Olson, E. N. (2007) Control of stress-dependent cardiac growth and gene expression by a microRNA. *Science* **316,** 575–579
38. Carè, A., Catalucci, D., Felicetti, F., Bonci, D., Addario, A., Gallo, P., Bang, M. L., Segnalini, P., Gu, Y., Dalton, N. D., Elia, L., Latronico, M. V., Høydal, M., Autore, C., Russo, M. A., Dorn, G. W., 2nd, Ellingsen, O., Ruiz-Lozano, P., Peterson, K. L., Croce, C. M., Peschle, C., and Condorelli, G. (2007) MicroRNA-133 controls cardiac hypertrophy. *Nat. Med.* **13,** 613–618
39. Najafi-Shoushtari, S. H., Kristo, F., Li, Y., Shioda, T., Cohen, D. E., Gerszten, R. E., and Näär, A. M. (2010) MicroRNA-33 and the SREBP host genes cooperate to control cholesterol homeostasis. *Science* **328,** 1566–1569
40. Esau, C., Davis, S., Murray, S. F., Yu, X. X., Pandey, S. K., Pear, M., Watts, L., Booten, S. L., Graham, M., McKay, R., Subramaniam, A., Propp, S., Lollo, B. A., Freier, S., Bennett, C. F., Bhanot, S., and Monia, B. P. (2006) miR-122 regulation of lipid metabolism revealed by *in vivo* antisense targeting. *Cell Metab.* **3,** 87–98
41. Milosevic, J., Pandit, K., Magister, M., Rabinovich, E., Ellwanger, D. C., Yu, G., Vuga, L. J., Weksler, B., Benos, P. V., Gibson, K. F., McMillan, M., Kahn, M., and Kaminski, N. (2012) Profibrotic role of miR-154 in pulmonary fibrosis. *Am. J. Respir. Cell Mol. Biol.* **47,** 879–887
42. Wang, K., Long, B., Zhou, L. Y., Liu, F., Zhou, Q. Y., Liu, C. Y., Fan, Y. Y., and Li, P. F. (2014) CARL lncRNA inhibits anoxia-induced mitochondrial fission and apoptosis in cardiomyocytes by impairing miR-539-dependent PHB2 down-regulation. *Nat. Commun.* **5,** 3596
43. Lee, Y. N., Brandal, S., Noel, P., Wentzel, E., Mendell, J. T., McDevitt, M. A., Kapur, R., Carter, M., Metcalfe, D. D., and Takemoto, C. M. (2011) KIT signaling regulates MITF expression through miRNAs in normal and malignant mast cell proliferation. *Blood* **117,** 3629–3640
44. Rodríguez-Meléndez, R., Cano, S., Méndez, S. T., and Velázquez, A. (2001) Biotin regulates the genetic expression of holocarboxylase synthetase and mitochondrial carboxylases in rats. *J. Nutr.* **131,** 1909–1913
45. Lima, V. V., Giachini, F. R., Choi, H., Carneiro, F. S., Carneiro, Z. N., Fortes, Z. B., Carvalho, M. H., Webb, R. C., and Tostes, R. C. (2009) Impaired vasodilator activity in deoxycorticosterone acetate-salt hypertension is associated with increased protein *O*-GlcNAcylation. *Hypertension* **53,** 166–174
46. Laczy, B., Marsh, S. A., Brocks, C. A., Wittmann, I., and Chatham, J. C. (2010) Inhibition of *O*-GlcNAcase in perfused rat hearts by NAG-thiazolines at the time of reperfusion is cardioprotective in an *O*-GlcNAc-dependent manner. *Am. J. Physiol. Heart Circ. Physiol.* **299,** H1715–H1727
47. Marsh, S. A., Dell'Italia, L. J., and Chatham, J. C. (2011) Activation of the hexosamine biosynthesis pathway and protein *O*-GlcNAcylation modulate hypertrophic and cell signaling pathways in cardiomyocytes from diabetic mice. *Amino Acids* **40,** 819–828
48. Deng, Y., Li, B., Liu, Y., Iqbal, K., Grundke-Iqbal, I., and Gong, C. X. (2009) Dysregulation of insulin signaling, glucose transporters, *O*-GlcNAcylation, and phosphorylation of tau and neurofilaments in the brain: implication for Alzheimer's disease. *Am. J. Pathol.* **175,** 2089–2098
49. Yuzwa, S. A., Macauley, M. S., Heinonen, J. E., Shan, X., Dennis, R. J., He, Y., Whitworth, G. E., Stubbs, K. A., McEachern, E. J., Davies, G. J., and Vocadlo, D. J. (2008) A potent mechanism-inspired *O*-GlcNAcase inhibitor that blocks phosphorylation of Tau *in vivo*. *Nat. Chem. Biol.* **4,** 483–490
50. Jacobsen, K. T., and Iverfeldt, K. (2011) *O*-GlcNAcylation increases non-amyloidogenic processing of the amyloid-β precursor protein (APP). *Biochem. Biophys. Res. Commun.* **404,** 882–886
51. Ma, Z., and Vosseller, K. (2013) *O*-GlcNAc in cancer biology. *Amino Acids* **45,** 719–733
52. Mi, W., Gu, Y., Han, C., Liu, H., Fan, Q., Zhang, X., Cong, Q., and Yu, W. (2011) *O*-GlcNAcylation is a novel regulator of lung and colon cancer malignancy. *Biochim. Biophys. Acta* **1812,** 514–519